

The magnonic limit of domain wall propagation in ferromagnetic nanotubes

Ming Yan, Christian Andreas, Attila Kákay, Felipe Garcia-Sanchez, and Riccardo Hertel
Institut für Festkörperforschung (IFF-9), Forschungszentrum Jülich GmbH, D-52428 Jülich, Germany
 (Dated: August 21, 2021)

We report a study on the field-driven propagation of vortex-like domain walls in ferromagnetic nanotubes. This particular geometry gives rise to a special feature of the static wall configuration, which significantly influences its dynamics. Unlike domain walls in flat strips, the left-right symmetry of domain wall propagation is broken. Furthermore, the domain wall velocity is not limited by the Walker breakdown. Under sufficiently large magnetic fields, the domain wall velocity reaches the velocity of spin waves (about 1000 m/s) and is thereafter connected with a direct emission of spin waves. The moving domain wall maintains its main structure but has characteristic spin-wave tails attached. The spatial profile of this topological soliton is determined by the spin-wave dispersion.

PACS numbers: 75.78.Cd, 75.60.Ch, 75.75.Jn, 75.30.Ds

The dynamic properties of objects moving in a medium often change dramatically as soon as their velocity exceeds the speed of waves propagating in the medium. Well-known examples thereof are the sonic barrier encountered when an object propagates through air at the speed of sound, or the Cherenkov radiation [1] which occurs when charged particles traverse a dielectric medium at velocities above the phase velocity of light. In both cases, the motion of the object is strongly damped above this limit – much stronger than below this critical velocity. If the object is accelerated, this critical velocity in fact acts as a ‘barrier’ above which a large part of the object’s energy is radiated into the medium in form of waves. For this reason, in the early times of aviation, the speed of sound was representing a limit of the achievable velocity of a plane.

In this letter we report on simulations predicting an analogous effect in ferromagnetic nanostructures. The role of the medium is here played by the ferromagnetic material, the propagating object is a domain wall (DW), and the radiation above the critical velocity occurs in the form of spin waves emitted by the DW. The magnonic limit of DW propagation was known in weak ferromagnets with a thickness in the μm scale [2] and analytically predicted for moving Bloch walls [3]. We here propose a particular geometry of magnetic nanostructures, a cylindrical tube, in which indeed a magnonic barrier occurs. A rather unique manner of spin-wave emission by supermagnonic DWs is discovered.

One major difficulty encountered when studying such effects in magnetic nanostructures is the very fast DW propagation required to reach the velocity of spin waves, which is in the order of about 1000 m/s for Permalloy (Py) – much higher than the typical DW speed in nanostructures. Such high velocities are problematic because the speed of DW is usually limited by the Walker breakdown [4], a micromagnetic instability occurring at a much lower critical velocity. The Walker breakdown is connected with a structural change of the DW and usually leads to an irregular, oscillatory DW motion [4, 5]. Al-

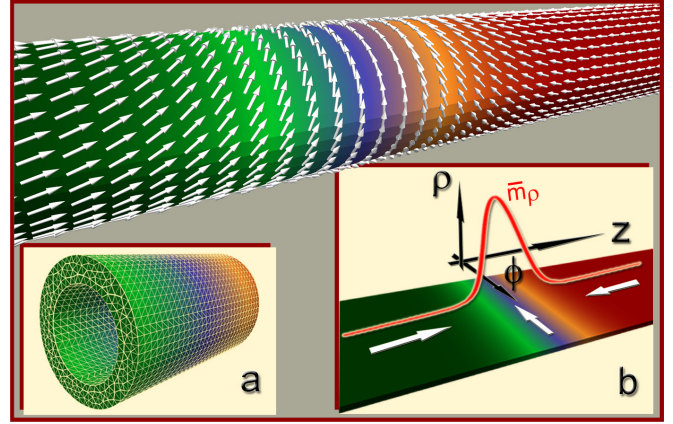


FIG. 1: A vortex-like DW formed in a $4 \mu m$ long Py tube with $40 nm$ inner diameter and $10 nm$ thickness. (a) A small section of the tube. (b) A flat strip obtained from ‘unrolling’ the curved surface of the tube with a cylindrical coordinate system. The white arrows indicate the magnetization near the DW. The red curve is the plot of \bar{m}_ρ near the DW indicating a non-zero radial component of the magnetization.

though it has recently been reported that in cylindrical nanowires a special type of massless DWs can develop which are not affected by the Walker limit [6], we quickly found that just because of the absence of mass this type of DW does not yield the desired interaction with spin waves. We then found that one could obtain both, supermagnonic DW velocities and non-vanishing DW mass, in the case of magnetic nanotubes. In such a tubular geometry, we also discovered an unexpected dynamic behavior of the vortex-like DWs: the propagation of these DWs breaks the left-right symmetry, which to our knowledge is taken for granted in any other case. This particular behavior, which will be discussed in more detail further below, leads to the occurrence of a favorable and unfavorable propagation direction – or DW chirality, the latter being just a different perspective on the same effect.

Similar to the case of thin strips [7], different types of

DWs can form in cylindrical wires [8]. With sufficiently large diameter, a vortex-like DW is energetically favorable, which contains a Bloch point in the middle. The Bloch point can be avoided by using a hollow cylindrical wire (a tube)[9, 10]. It is worthwhile to notice that a nanotube can be considered as a curved thin strip without lateral boundary. As we will show later, both features of the tube, the curvature of the surface and the periodic boundary condition, have significant influences on the DW dynamics. Figure 1 shows the configuration of a vortex-like head-to-head (h2h) DW formed in a $4 \mu\text{m}$ long Py tube with 40 nm inner diameter and 10 nm thickness. The direction of the local magnetization is indicated by a unit vector \vec{m} in a cylindrical coordinate system with the z axis along the tube. In the DW region, the magnetization circles around the tube and forms a coreless vortex. Such a DW is analogous to a transverse DW in thin strips, which can be displayed by artificially 'unrolling' the tube into a flat thin strip as shown in Fig. 1b. Obviously, there exist two energetically degenerate configurations of the DW with opposite vorticity ($\pm m_\phi$). This corresponds to the two equivalent orientations of the transverse DWs along the width direction in flat strips. The curvature of the tube, however, has an important consequence on the DW configuration. Unlike a transverse DW in flat strips, where the magnetization lies perfectly in plane, the vortex-like h2h DW in the tubes has a small positive radial component of the magnetization (m_ρ). This is illustrated by the plot of the averaged m_ρ over each cross section of the tube (\bar{m}_ρ) near the DW in Fig. 1b. The presence of the non-zero m_ρ is to reduce one major source of the DW energy, the volume charge generated in the DW region. The volume charge density is proportional to the divergence of the magnetization field. In cylindrical coordinates, the divergence of the magnetization vector \vec{m} is given by

$$\vec{\nabla} \cdot \vec{m} = \frac{m_\rho}{\rho} + \frac{\partial m_\rho}{\partial \rho} + \frac{1}{\rho} \frac{\partial m_\phi}{\partial \phi} + \frac{\partial m_z}{\partial z}. \quad (1)$$

The last term is negative for h2h DWs and positive for tail-to-tail (t2t) DWs. Clearly, by having a positive m_ρ , the total volume charge of the h2h DWs is compensated. For the same reason, a negative m_ρ should appear for t2t DWs in nanotubes, which is confirmed in our simulations.

The magnetization dynamics of the DW is described by the Landau-Lifshitz-Gilbert equation :

$$\frac{d\vec{M}}{dt} = -\gamma \vec{M} \times \vec{H}_{\text{eff}} + \frac{\alpha}{M_s} \left[\vec{M} \times \frac{d\vec{M}}{dt} \right], \quad (2)$$

where \vec{M} is the local magnetization, M_s the saturation magnetization, γ the gyromagnetic ratio, \vec{H}_{eff} the effective field, α the Gilbert damping factor. In our simulations, Eq. 2 is solved numerically using a finite-element method [11]. Typical material parameters of Py, $\mu_0 M_s = 1 \text{ T}$ (saturation magnetization) and exchange

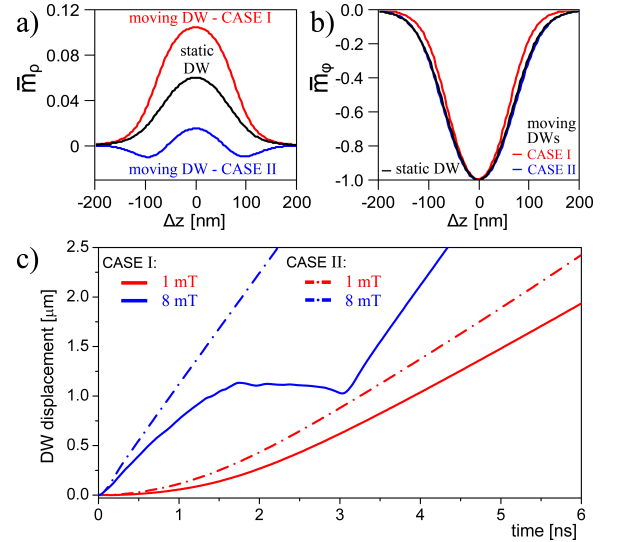


FIG. 2: Comparison of the configuration between a static DW and moving DWs in both case I and II by plotting \bar{m}_ρ and \bar{m}_ϕ in (a) and (b) respectively. The moving DWs are driven by a 1 mT field in opposite directions ($+z$ corresponding to case I and $-z$ to case II). (c) DW displacement versus time in the two cases driven by two different fields.

constant $A = 1.3 \times 10^{-11} \text{ J/m}$ are used. The sample volume is discretized into irregular tetrahedrons with cell size of about 3 nm . The damping factor is fixed to 0.02.

To drive the DW, a magnetic field is applied along the tube. In flat strips, changing the orientation of the DW or the field direction (left or right) does not affect the DW dynamics. It is, however, not the case in the tube. This is because of the non-zero m_ρ of the static DW. Considering the torque exerted by the field on the DW, which is given by the cross product of the field and magnetization, two situations can be distinguished. In one case (I), the torque tends to increase the already existing m_ρ , while suppressing it in the other (case II). In those two cases, the DW should therefore be distorted differently and thereby move differently as well. This symmetry break is indeed observed in the simulations of the DW motion driven by fields applied in opposite directions. Given the vorticity of the DW shown in Fig. 1, the field in $+z$ corresponds to case I and $-z$ to case II. Figure. 2a shows the expected enhancement and compression of \bar{m}_ρ for the moving DW in case I and II respectively. The symmetry-break effect is already remarkable for a 1 mT applied field. The plot of \bar{m}_ϕ in Fig. 2b shows that the moving DW width is also different in case I and II. The displacement of the DW as a function of time is plotted in Fig. 2c for two field values (1 and 8 mT). In case II, the DW always reaches a constant speed after a period of acceleration. In case I, the motion is more complex. At low fields, the DW reaches a constant speed, which is always lower than that in case II for the same field value.

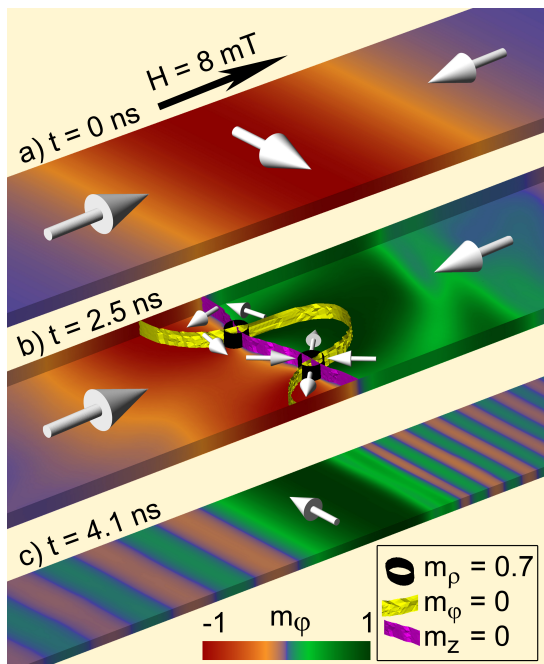


FIG. 3: Snapshots of the DW configuration before, during and after a breakdown occurring in case I. For better visualization, the flat strip after ‘unrolling’ is shown. The magnetization is indicated by both the color and white arrows. In (b), only the bottom surface and the lateral edges of the strip are shown. Three isosurfaces are utilized to locate the vortex-antivortex cores. In (c), the view of the DW is zoomed out to show the spin-wave tails.

This velocity difference can be attributed to the different DW width during its motion in case I and II as shown in Fig. 2b, because the DW velocity is proportional to the DW width [4]. Above a critical field (about 5 mT), the motion shows a ‘three-stage’ behavior. In the first stage, the DW moves with a constant speed. In the second stage, the average velocity of the DW becomes close to zero. In the third stage, the DW resumes its motion and acquires a higher speed compared to the first stage. Notice that the DW speed of the third stage is exactly the same as that in case II for the same field value.

The ‘three-stage’ motion of the DW in case I is caused by a breakdown process, which is demonstrated in Fig. 3. For better visualization, the ‘unrolled’ tube is shown as a flat strip. As mentioned before, in case I, the initial \bar{m}_ρ of the DW is further increased by the field torque. At a critical field, this distortion (large radial component of the magnetization) leads to the collapse of the DW. This breakdown process is characterized by the nucleation of a vortex-antivortex pair. The vortex and anti-vortex cores are indicated by the crossings of two isosurfaces ($m_z = 0$ and $m_\phi = 0$) and isosurface $m_\rho = 0.7$ in Fig. 3b. After the pair is created, they move away from each other and eventually meet on the other side of the tube and

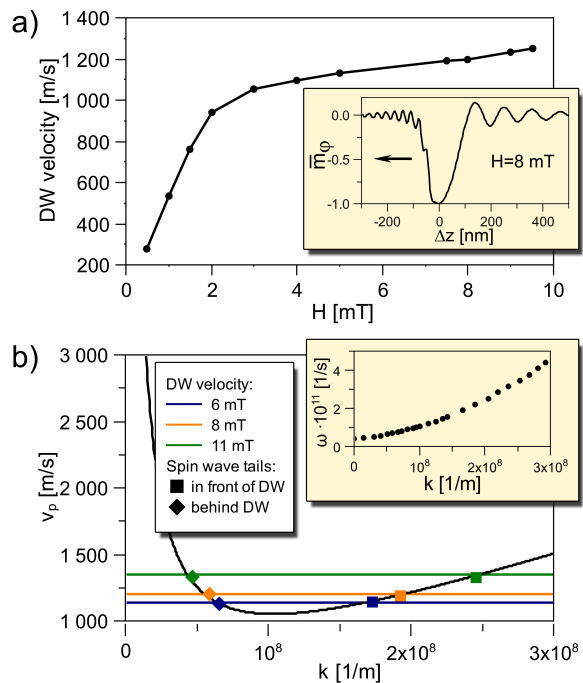


FIG. 4: (a) DW mobility of the nanotube in case II. Inset: A snapshot of the moving DW configuration by plotting \bar{m}_ϕ near the DW. The arrow indicates the moving direction of the DW driven by a 8 mT field. (b) Spin-wave phase velocity as a function of wave vector extracted from its dispersion (inset). Spin-wave tails of the moving DWs driven by three different fields are compared to corresponding eigen modes.

annihilate. During this process, the DW motion is very complex. The DW stops to move or even moves backward momentarily. This velocity drop is similar to the Walker breakdown occurring in flat strips. Notice that after the annihilation of the pair, the DW reverses its vorticity as shown in Fig. 3c and its motion thereafter switches from case I to II. This breakdown process in the tube differs from that in flat strips mainly in two aspects. First, the breakdown in the tube involves a vortex-antivortex pair instead of just a single vortex or anti-vortex as in flat strips [5]. This is attributed to the lack of lateral boundaries in the tube and the requirement to conserve the winding number. A similar process of vortex-antivortex pair creation and annihilation has been well understood in vortex dynamics [12, 13]. Because the energy needed to create a vortex-antivortex pair is higher than that for a single vortex/anti-vortex, the breakdown in tubes should have a higher threshold than that in flat strips. Our simulations confirmed this (data not shown in this paper). Secondly, the breakdown process in the tube is not repetitive as in thin strips. This is due to the symmetry-break of the DW motion in the tube as discussed before.

We now focus on the DW motion in case II. In this case, the initial \bar{m}_ρ of the DW is suppressed by the field torque. Therefore, the occurring of the breakdown trig-

gered by a vortex-antivortex pair creation is expected to be more difficult compared to case I. In fact, the breakdown is never observed in case II. At each field value in our studied range, the DW moves with a nearly constant speed. The DW velocity as a function of field is plotted in Fig. 4a. At low fields, the DW velocity is linearly dependent on the field. Above a critical velocity (about 1000 m/s), the DW velocity curve shows a dramatic change of its slope. This mobility change is found to be resulting from a direct emission of spin waves by the DW. A typical snapshot of the spin waves is shown in Fig. 3c and the inset of Fig. 4a. One can see that spin waves are emitted both in front of and behind the DW. Both of them have well-defined yet different wave length. This characteristic manner of spin-wave emission is different from that of the Walker breakdown, in which spin waves with a broad spectrum are excited by the abrupt change of the DW structure. The DW structure in this case remains nearly the same except for the spin-wave tails. The whole structure is non-dispersive and moves in a dynamic equilibrium [14]. From topological point of view, this moving DW is a supermagnonic soliton with an asymmetric spatial structure. For a further understanding, we numerically calculated the spin-wave dispersion of the tube as shown in the inset of Fig. 4b. In principle, the presence of a DW and the external field influence the dispersion. Because of the relatively small field applied in our study, the field effect on the dispersion is neglected. A DW can cause a phase shift to spin waves passing through [15, 16], which is not important for our purpose. The phase velocity (v_p) of the spin waves shown in Fig. 4b is then extracted from the dispersion. One immediately sees that v_p has a minimum around 1000 m/s , which coincides with the critical velocity of the DW to emit spin waves. In case I, the breakdown occurs at a critical velocity around 800 m/s , which is less than this minimum spin-wave velocity. One also sees that there exist two spin-wave modes with the same v_p . For a supermagnonic DW with a certain velocity v , its two spin-wave tails are found to originate from the two eigen modes sharing the same v_p that is equal to v . This is shown in Fig. 4b by the excellent match between the spin-wave tails of the DW and the corresponding spin-wave eigen modes at three different field values. The wave length and frequency of the spin-wave tails are measured from the simulations. Because v_p of the spin-wave tails is the same as the DW velocity, the spin waves have zero frequency in the moving frame of the DW [14]. The spin waves are therefore emitted because of soft-mode instability [3], which are not the 'wake' of a moving DW proposed in another DW motion damping mechanism [17]. Note that after the whole structure reaches a dynamic equilibrium, the spin-wave tails with relatively short wave length and high frequency always appear in front of the DW. This is due to the dispersion of the wave package occurring in its initial stage because of the different group velocity of the two spin-

wave modes. The emission of spin waves transfers energy stored in the DW and therefore hinders the further distortion of the DW. Consequently, the DW mobility is reduced. We point out that the dynamics of the DW in nanotubes is not thickness specific. Tubes with three different inner diameters, 40, 30, and 10 nm , have been studied and the same physics is revealed.

To conclude, we numerically demonstrate that a magnonic barrier of DW propagation in ferromagnetic nanostructures can occur in a tubular geometry. This is indicated by the significant reduction of the DW mobility and strong emission of spin waves by the moving DW when the DW velocity exceeds the spin-wave velocity. The characteristic manner of spin-wave emission is understood in terms of its dispersion. In addition, the curvature of the tube also causes the break of the left-right symmetry of the DW propagation. Since fabrication of such ferromagnetic nanotubes is feasible [18, 19], it is promising to experimentally verify these findings.

-
- [1] P. A. Cherenkov, Doklady Akademii Nauk SSSR **2**, 451 (1934).
 - [2] V. G. Bar'yakhtar, M. V. Chetkin, B. A. Ivanov, and S. N. Gadetskii, in *Dynamics of Topological Magnetic Solitons. Experiment and Theory*, (Springer, Berlin, 1994), Chapt. 4.
 - [3] D. Bouzidi, and H. Suhl, Phys. Rev. Lett. **65**, 002587 (1990).
 - [4] N.L. Schryer, and L.R. Walker, J. Appl. Phys. **45**, 5406 (1974).
 - [5] Y. Nakatani, A. Thiaville, and J. Miltat, Nature Mater. **2**, 521 (2003).
 - [6] M. Yan, A. Kákay, S. Gliga, and R. Hertel, Phys. Rev. Lett. **104**, 057201 (2010).
 - [7] R. D. McMichael, and M. J. Donahue, IEEE Trans. Magn. **33**, 4167 (1997).
 - [8] R. Hertel, J. Magn. Magn. Mater. **249**, 251 (2002).
 - [9] R. Hertel, and J. Kirschner, J. Magn. Magn. Mater. **278**, 291 (2004).
 - [10] P. Landeros, O. J. Suarez, A. Cuchillo, and P. Vargas, Phys. Rev. B **79**, 024404 (2009).
 - [11] R. Hertel, J. Appl. Phys. **90**, 5752 (2001).
 - [12] R. Hertel, and C. M. Schneider, Phys. Rev. Lett. **97**, 177202 (2006).
 - [13] R. Hertel, S. Gliga, M. Fähnle, and C. M. Schneider, Phys. Rev. Lett. **98**, 117201 (2007).
 - [14] See EPAPS Document No.xxxxx for two movies of spin waves emitted by a moving DW.
 - [15] R. Hertel, W. Wulfhekel, and J. Kirschner, Phys. Rev. Lett. **93**, 257202 (2004).
 - [16] A.L. González, P. Landeros, and Álvaro S. Núñez, J. Magn. Magn. Mater. **320**, 530 (2010).
 - [17] R. Wieser, E. Y. Vedmedenko, and R. Wiesendanger, Phys. Rev. B **81**, 024405 (2010).
 - [18] K. Nielsch, F. J. Castaño, C. A. Ross, and R. Krishnan, J. Appl. Phys. **98**, 034318 (2005).
 - [19] K. Nielsch, J. Choi, K. Schwirn, R. B. Wehrspohn, and U. Gösele, Nano Lett. **2**, 677 (2005).